

## Investigation of the mica x-ray absorption near-edge structure spectral features at the Al K-edge

This article has been downloaded from IOPscience. Please scroll down to see the full text article.

2003 J. Phys.: Condens. Matter 15 7139

(<http://iopscience.iop.org/0953-8984/15/41/021>)

View [the table of contents for this issue](#), or go to the [journal homepage](#) for more

Download details:

IP Address: 171.66.16.125

The article was downloaded on 19/05/2010 at 15:20

Please note that [terms and conditions apply](#).

## Investigation of the mica x-ray absorption near-edge structure spectral features at the Al K-edge

Ziyu Wu<sup>1,2,4</sup>, A Marcelli<sup>2</sup>, G Cibin<sup>2</sup>, A Mottana<sup>2,3</sup> and G Della Ventura<sup>2,3</sup>

<sup>1</sup> Beijing Synchrotron Radiation Facility, Institute of High Energy Physics, Chinese Academy of Sciences, PO Box 918, Beijing 100039, People's Republic of China

<sup>2</sup> Laboratori Nazionali di Frascati, Istituto Nazionale di Fisica Nucleare, Via Enrico Fermi 40, 00044 Frascati, Italy

<sup>3</sup> Dipartimento di Scienze Geologiche, Universita' Roma Tre, Largo Murialdo 1, 00146 Roma, Italy

E-mail: wuzy@ihep.ac.cn

Received 2 June 2003

Published 3 October 2003

Online at [stacks.iop.org/JPhysCM/15/7139](http://stacks.iop.org/JPhysCM/15/7139)

### Abstract

Near-edge features of Al x-ray absorption near-edge structure (XANES) spectra in aluminosilicate compounds with mixed coordination number are usually assigned to a fourfold coordinated site contribution followed by a sixfold coordinated site contribution that is displaced towards higher energy because of the increasing ligand nucleus potentials, neglecting possible contributions due to bond distance variations and local geometrical distortion. Here we present and discuss the Al K-edge XANES spectra of synthetic micas with either fourfold coordinated Al (phlogopite), or with sixfold coordinated Al (polyolithionite), as well as with mixed coordination (preiswerkite). Multiple scattering simulations of XANES spectra demonstrate that octahedral contributions may overlap the tetrahedral ones so that the lower energy structures in mixed coordination compounds may be associated with the octahedral sites. This unexpected behaviour can be described as due to the effect of a significant reduction of the ligand field strength (i.e. large local distortion and Al–O bond distances).

Recently, there has been intense activity in x-ray absorption near-edge structure (XANES) investigations of the valence, coordination number (CN) and bond length of minerals of the earth's crust on well characterized systems such as: micas, olivines, feldspars, garnets, etc as well as on some aluminosilicate melts and glasses. This is due, at least in part, to the consistent growth of XANES spectroscopy, from both the theoretical and experimental point of view [1]. Indeed, this modern technique allows one to directly probe and characterize the

<sup>4</sup> Author to whom any correspondence should be addressed.

chemical composition, site symmetry and other structural information on the selected atomic site (photoabsorber) independently upon other atoms present in the studied material.

Among the compounds of interest, attention has been recently devoted to mica minerals. Micas are abundant minerals on earth and are also structurally significant because they are characterized by layered structures consisting of sheets of tetrahedra and octahedra cornered by O or OH that alternate with sheets centred by very large alkali and alkaline-earth atoms that are loosely coordinating only the O of the tetrahedra. Let us forget for the time being about other major atoms such as Si, Mg and K, and rather concentrate on Al, one of the most significant constituents of these minerals, which may occur either in the tetrahedra or in the octahedra only, or in both these coordination polyhedra simultaneously. The gross features in XANES spectra at the Al K-edge are dominated by the first coordination sphere around the absorber i.e. by the surrounding four and/or six O atoms. In the experimental XANES spectra recorded on micas with Al in mixed coordination, the main edge consists of two or three peaks [2, 3]. Usually these peaks are assigned to either the tetrahedral or octahedral sites, respectively, in terms of ligand electronegativity. However, without a careful and accurate theoretical analysis any approach of this kind can be misleading since:

- (1) many investigations utilize the average K-edge position, neglecting possible variations in the coordination polyhedron bonding distances (i.e. large distortion) that indeed affect the edge features, and
- (2) the edge position depends also on the chemical environment, such as the next-neighbour O–H units and even higher-shell cations. As a matter of fact, recent investigations carried out on the atomic structure of model compounds sometimes show a good deal of disagreement [4, 5].

In order to determine the relationships between type of first coordination shell and energy position of the relevant edge feature, it is useful to analyse the spectroscopic properties in conjunction with a detailed full multiple scattering (MS) analysis. This strategy has proved successful in the interpretation of many systems [1, 6–9]. In this paper we present experimental data and *ab initio* full MS calculations of the XANES spectra at the Al K-edge for three micas: phlogopite (Phl), containing fourfold coordinated Al sites only, polyolithionite (Pol), containing Al in sixfold coordinated sites only, and another mica having Al in both (i.e. 4 + 6) coordinations, preiswerkite (Pwk). Their Al K-edge spectra had been previously interpreted according to the ligand electronegativity model by the fingerprinting method, i.e. by comparison with the spectra of model compounds albite (CN = 4) and grossular (CN = 6) [2]. Results were satisfactory in the case of the micas with one type of Al only, but not clear in the case where both Al types were present. This research and the resulting data suggest a new kind of relationships i.e. the lower energy structure in the Al K-edge XANES spectrum of our mixed coordination compound has to be attributed to the octahedral sites, or it originates mainly from the contribution of the octahedral sites. This may be due of the reduced ligand field strength owing to the rather large Al–O bond length distribution i.e. to polyhedral distortion. This behaviour is supported by the analysis of the spectra of certain Fe<sup>2+</sup> and Ti<sup>4+</sup> bearing compounds [10, 11].

All three micas here discussed are synthetic materials whose preparation procedure is described in [2]. They were chosen to cover a wide spectrum of Al contents: (1) Al in the tetrahedral sheet only (Phl), (2) Al in the octahedral sheet only (Pol), and (3) Al in both sheets simultaneously (Pwk). X-ray absorption fine-structure (XAFS) experiments were carried out at SSRL (Stanford, CA, USA), with the SPEAR storage ring operating at energy 3 GeV and injection current 100 mA, at beam line SB03-3, which is equipped with the JUMBO monochromator of the double-crystal type consisting of two plates of a single YB<sub>66</sub> crystal

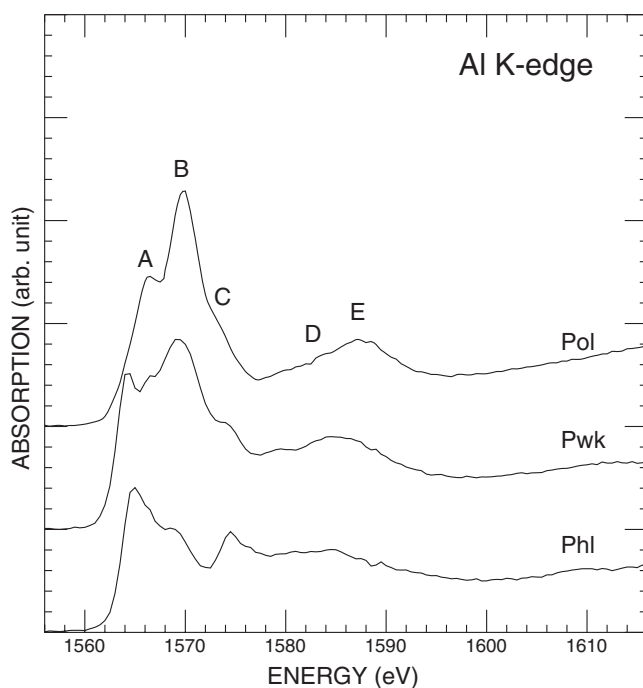


**Figure 1.** Experimental XANES spectra at the K-edge of: Phl containing  $^{27}\text{Al}$ , Pol containing  $^{27}\text{Al}$ , and Pwk containing Al in both coordinations.

cut along the (400) plane, with resolution less than 0.55 eV. Spectra were recorded in the total electron yield (TEY) mode by scanning the Al K-edge from 1540 to 1690 eV in steps of 0.3 eV. They were corrected for background contribution from lower energy absorption edges by linear fitting of the baseline, and normalized in energy to + 60 eV from the first inflection of the edge i.e. at the uppermost energy value for XANES [12].

The experimental spectra presented in figure 1 show a dramatic change in the major features at the Al K-edge as a function of the different Al coordination states. Pol and Phl both contain one Al atom per formula unit. However, in the Pol system the Al atoms are located in the octahedral sheet [13], whereas in Phl Al is in the tetrahedral sheet [14, 15]. The two minerals have XANES spectra showing a major feature followed by several minor ones, but they differ both in energy position and in the relative intensities. By contrast, Pwk contains one Al in the octahedral sheet and two Al in the tetrahedral sheet [16] and exhibits three peaks at the edge that have fairly similar intensities.

The XANES spectra have been computed using full MS theory and SW packages described elsewhere [9, 17–21]. In the muffin-tin model and one-electron approximation, the local density potentials for the system have been constructed according to the Mattheiss prescription [22] by superposition of neutral atomic charge densities using the Clementi–Roetti [23] basis set tables. For the exchange–correlation part of the potential, for practical reasons, we used the energy-independent  $X_\alpha$  potential with  $\alpha$  equal to 0.60 for the excited Al atom. In order to simulate the charge relaxation around the core hole, we selected the well tested screened  $Z + 1$  approximation final state rule [21], which consists of taking into account the orbitals of the ( $Z + 1$ ) atom and constructing the charge density by using the excited electronic configuration of the photoabsorber with the core electron promoted to an empty

orbital. In metallic and (nearly) covalent systems this method is known to provide a quite reasonable approximation of the relaxed charge distributions as obtained by self-consistent-field (SCF) calculations, at least within the muffin-tin model and for the purpose of calculating absorption spectra in the MS scheme, in the sense that the two methods yield very similar spectra. However, if one is interested in the near-edge region of the spectrum, one should perform a self-consistent calculation of the cluster under investigation. As is quite well known, with standard computational systems it is almost impossible to built self-consistent potentials for clusters with a large (about 20) number of atoms. In our case we actually calculated an SCF potential and a charge density for a small cluster around the photoabsorber and embedded this cluster into the larger one for the MS simulation. This method has been considered because the use of SCF potentials only affects the first 5–10 eV above the edge [24]. Actually in this energy region localized molecular states contribute significantly to the total cross section [25]. Due to their spatial localization, they are only sensitive to the details of the potentials of the absorber and its first neighbours. The calculated spectra are further convoluted with a Lorentzian shaped function with a full width  $\Gamma_h = 0.42$  eV [26] to account for the core hole lifetime and  $\Gamma_{\text{exp}} = 0.55$  eV for the experimental resolution. We have chosen the muffin-tin radii according to Norman's criterion [27] and allowed a 10% overlap between contiguous spheres to simulate the atomic bond. The  $z$  axis in all our calculations is along the  $c$  axis of the compound.

The conventional strategy for calculating Al XANES spectra would be to construct cluster models with Al in tetrahedrons and octahedrons, respectively for Phl and Pol, using the Al–O bond distances determined with the best x-ray diffraction (XRD) refinements available and with clusters of increasing size until convergence is achieved i.e. until two successive calculations do not show substantial variation. Usually convergence is reached after adding atoms up to the sixth or seventh shell [28]. However, we decided to test this strategy starting from its initial assumption, because XRD sees an average cation–anion distance only, whereas XANES is essentially a local probe. Therefore, we checked the effect on the edge position of first the bond length and then the coordination i.e. the number of nearest neighbours. We also checked how a change of the coordinated anion from O (oxygen) to OH (hydroxyl) would affect the edge position for the coordinating octahedral Al cation.

In order to show how much the edge peak position depends upon bond length, we present in figure 2 a series of SCF–MS calculated spectra using simplified cluster models, a tetrahedron and an octahedron, both as a function of the bond distances. A clear tendency of the edge to shift towards lower energies with increasing Al–O bond length is observed. The rate of change is about  $20.4 \text{ eV } \text{\AA}^{-1}$  for fourfold coordinated Al over the range 1.70–1.80  $\text{\AA}$  and about  $13.6 \text{ eV } \text{\AA}^{-1}$  for sixfold coordinated Al over the range 1.90–2.00  $\text{\AA}$ . These rates are similar to those experimentally observed for Ti K-edge features [11] and Si K-edge features [29].

In figures 3(a) and (b) we present calculations of the idealized tetrahedron and octahedron models (indicated in the figures by IM) using two different potentials:  $Z + 1$  and SCF. In figures 3(c) and (d) we present similar calculations that take into account all the distortions observed in the real crystal structures of Pwk (indicated in the figures by RS). Figure 3 clearly shows that the main peak position of the octahedral cluster is at a lower energy than the tetrahedral one, even with the SCF potential, thus indicating that the observed 'anomalous chemical shift' is mainly due to the larger distortion around the photoabsorber. On the other hand, the results obtained for the ideal model (IM) exhibit a net shift of about 2.2 eV (the fourfold coordinated site contribution being followed by the sixfold coordinated site contribution). These XANES calculations at the Al K-edge suggest that structural distortion plays an important role in determining the details of the transition features of compounds with mixed coordination.

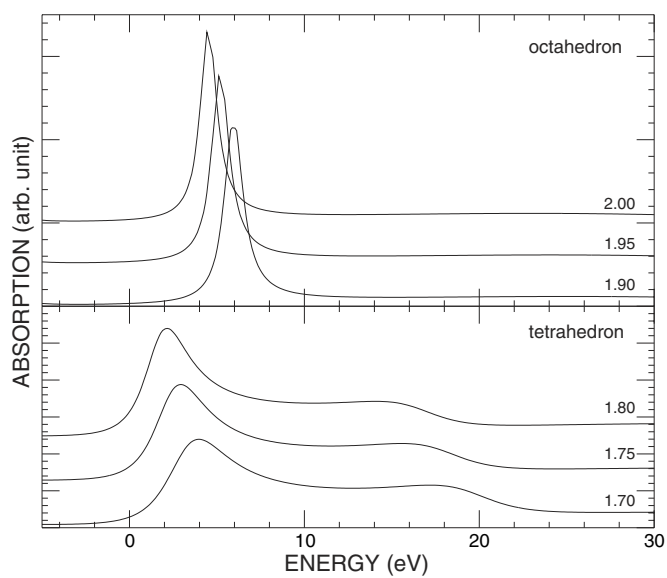


**Figure 2.** Simplified self-consistent model calculations at the Al K-edge in tetrahedral and octahedral clusters, as a function of the bond distance.

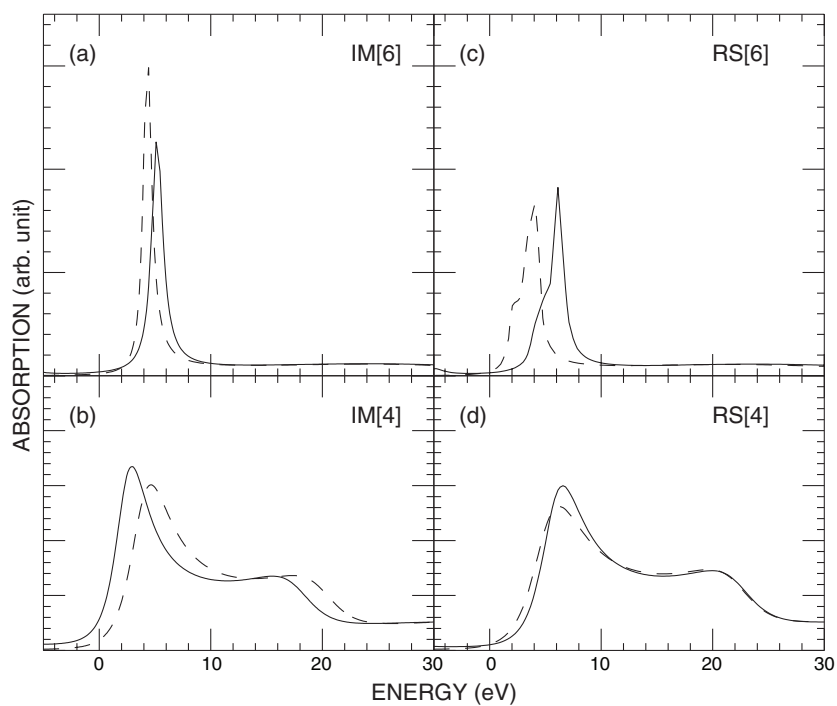


**Figure 3.** (a) Ideal octahedral model calculations ( $d = 1.95 \text{ \AA}$ ), (b) ideal tetrahedral model calculations ( $d = 1.75 \text{ \AA}$ ), (c) real sixfold cluster calculations in Pwk, and (d) real fourfold cluster calculations in Pwk, using two different potentials: SCF (solid curve) and  $Z + 1$  (dashed curve).

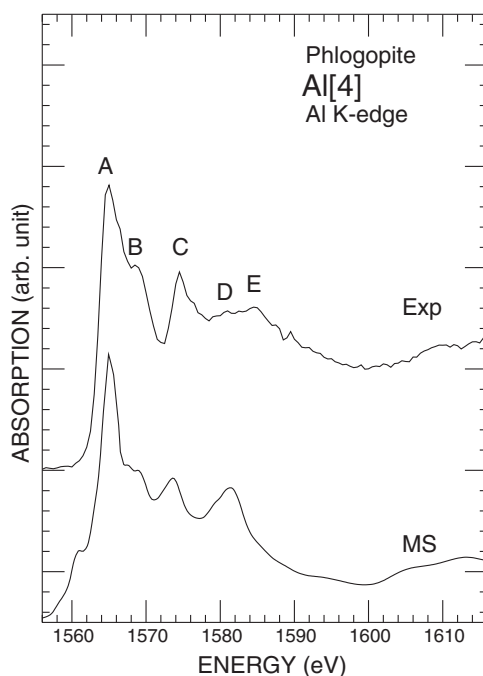


**Figure 4.** Comparison of experimental and theoretical MS simulations at the Al K-edge in Phl.

In figure 4 we present the MS calculation at the Al K-edge for Phl, along with its experimental spectrum. These calculated and observed edge structures are, in fact, quite similar to those observed in other minerals having fourfold coordinated Al, such as albite [2, 4]. They consist of a strong single-edge maximum (A), which is attributed to  $1s-3p$  transitions, and at least other four well defined features (MS contributions). All these experimental features are reproduced well using an 80-atom cluster extending to about 6.0 Å from the centre of the cluster.

The related spectrum of sixfold coordinated Al in Pol is reported in figure 5 along with its MS computation, which reproduces the experimental spectrum very closely. There are four features in the first 20 eV. Two resonances are clearly resolved at the main edge, which resembles the spectrum of octahedral Al in grossular [2, 28]. The experimental and calculated Al K-edge XANES spectra of Phl ( $^{27}\text{Al}$ ) and those of Pol ( $^{27}\text{Al}$ ) differ in two major characteristics: (1) the negative shift in the energy position of the edge (about  $-2$  eV), and (2) the intensity ratio of the main peak. The negative shift of Phl is certainly due to its lower Al CN. This shift is consistent, and it is a reliable basis for the fingerprinting method.

Figure 6 shows the experimental and calculated Al XANES spectra for Pwk, a mica having Al in two coordination states (one octahedral  $^{6}\text{Al}$  and two tetrahedral  $^{4}\text{Al}$ ). We first calculated the convergent 91-atom cluster for each site, then we combined them in the proportion  $1^{6}\text{Al} + 2^{4}\text{Al}$ . Peak A originates from the O-site contribution, peak B from a superposition of contributions from both sites, while C is dominated by the T-site contribution. This is not surprising if one notices that, according to the crystal structure determination, the Al–O bond lengths are about 2.02 and 1.69 Å for octahedral and tetrahedral sites, respectively. The large octahedral bond distance shifts the edge position towards lower energy (see figure 2), whereas the opposite occurs for Al clusters having short length tetrahedral sites. Furthermore

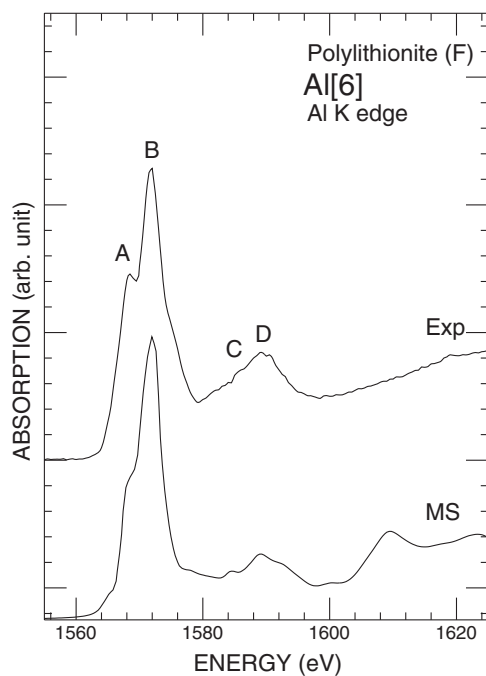


Figure 5. Comparison of experimental and theoretical MS simulations at the Al K-edge in Pol.

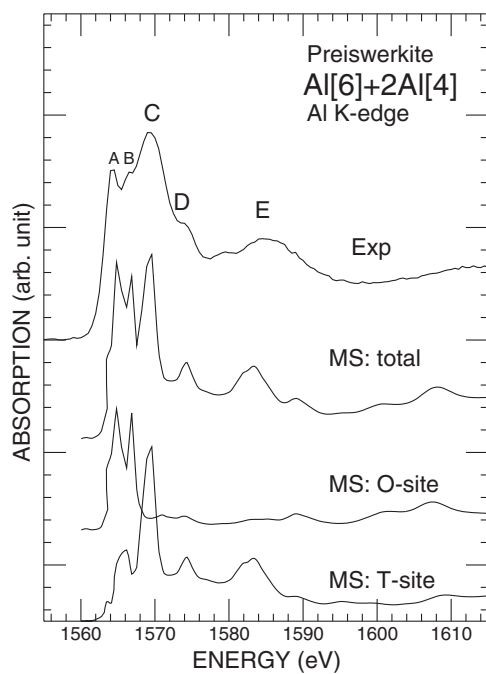
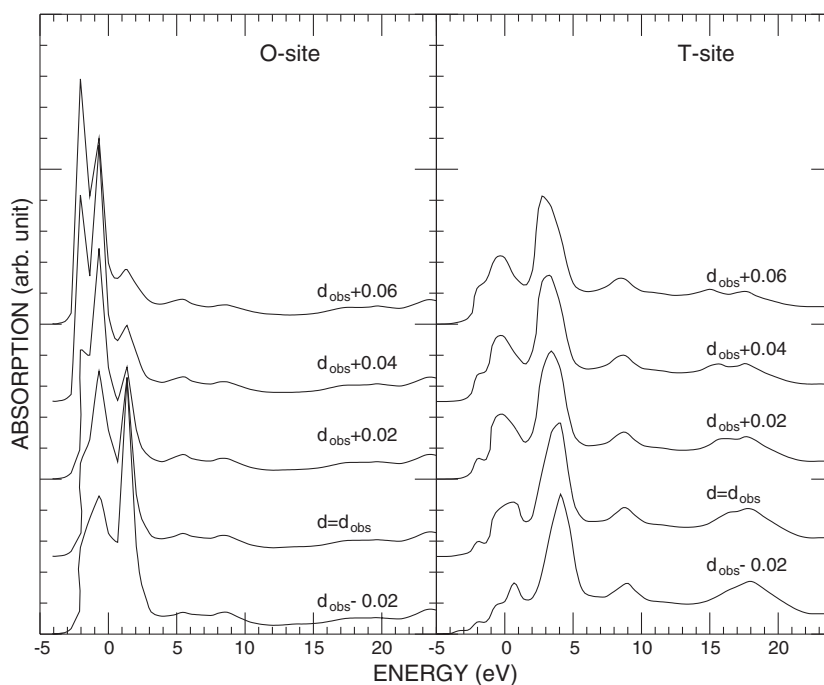


Figure 6. Pwk—comparison of theoretical Al K-edge spectra for the two different sites and their combination with experimental data.





**Figure 7.** Pwk—comparison of theoretical Al K-edge spectra for the two different sites using the same atomic cluster as figure 6, but different distances (in Å) between photoabsorber and the first oxygen shell.

the larger distortion of the tetrahedral site also shifts the peak position toward higher energy by more than 2.0 eV [6]. As a matter of fact, MS calculations would indicate that all features are determined by the superposition of contributions from both sites. However, peaks A and B are mainly, but not only, of octahedral origin, while C is only due to tetrahedral contributions. Another strong piece of evidence to support the above assignments comes from the inspection of spectral feature E (figure 6), which has the typical shape of the tetrahedral Al XANES spectrum, in contrast to the octahedral one that is flat in this energy range.

To summarize, in figure 7 we present the calculated spectra of one tetrahedron and one octahedron for Pwk using the same atomic clusters used in figure 6. Here  $d = d_{\text{obs}}$  i.e. the actual sizes of the two polyhedra as determined by SC-XRD [16] are used:  $d_{[6]Al-O} = 2.02 \text{ \AA}$  and  $d_{[4]Al-O} = 1.69 \text{ \AA}$ . A stepwise increase of the size of the nearest octahedron by 0.02 Å enhances the first peak in the simulation. It becomes the strongest peak, but it does not affect the position of the inflection point. The main peak position appears to be at about 3.4 eV lower energy than expected. By contrast, a stepwise increase of the tetrahedral size enhances only slightly the entire spectrum and makes its edge broader (in the lower energy part) except for the features at 20 eV above the edge onset. These data confirm the assignment to  $^{61}\text{Al}$  of the origin of the first feature of the Al K-edge in our mixed coordination compound Pwk.

We also carried out a further test, albeit preliminary, on the changes induced by O–H bonds onto the  $^{61}\text{Al}$  spectrum. This test is important because of the special configuration of the Al coordination polyhedron in micas: it consists of four O anions in common with the tetrahedral sheet plus two OH located at the centre of the ensuing O hexagonal network. The formation of the O–H bond reduces the total electronegativity of the Al–O bonds in two opposite directions,

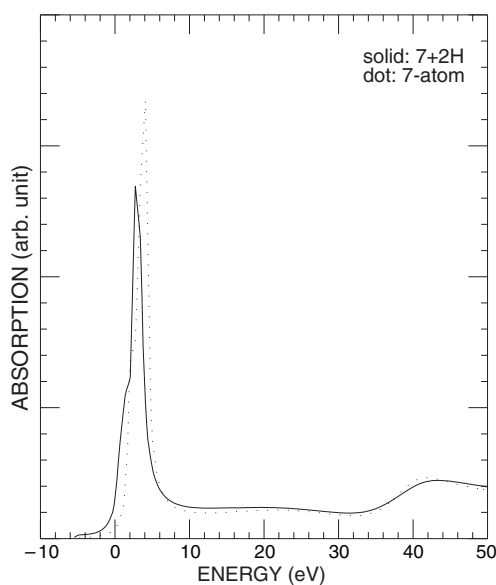


**Figure 8.** Comparison of MS calculations at the Al K-edge for a simplified Al cluster (e.g. Al + 6O) with (solid) and without hydrogen (dotted).

and leads to an edge shift towards lower energies, as shown in figure 8. Here we present the calculations for a simplified small cluster that contains only a first coordination oxygen shell with one O anion linked to hydrogen. Theory shows that formation of the O–H bond shifts the edge position towards low energy (about 1.0 eV), and decreases the intensity of the main edge with a concomitant formation of new states near the Fermi level. This finding supports our previous assignment and is in agreement with data available in the literature [30–32]. Actually, increasing bond length, O–H bond formation and large site distortion, on one side, and increasing CN, on the other side, are competitive mechanisms for the formation of the Al K-edge.

In conclusion, a detailed experimental and theoretical investigation of the Al K-edge XANES has been performed on three different micas that contain Al in different coordinations. The present study characterizes the Al signature in the octahedral and tetrahedral coordinations. However, coordination is not the only factor that affects the edge position. Bond length, OH formation and, more importantly, site distortion have to be considered. Moreover, it should be noted that tetrahedral bond lengths determined by the x-ray methods are only average values taking into account all Al + Si sites; in fact, for a given Al atom the local bond length should be expected to be different from the average value, but the magnitude of this difference has large uncertainties. XANES, on the other hand, probes the local environment i.e. the first coordination shells, so that the spectra represent the weighted sum of all these sites without averaging them over a long distance.

The anomalous chemical shift contribution to the Al K-edge peak indicates that the fingerprinting technique based on the extrapolation of the results of the fourfold and sixfold structures in the spectra of model compounds is reliable only if combined with a theoretical analysis. This is particularly true for compounds relevant in mineralogy and geochemistry, where atoms such as Al occur in different coordination sites and with different bond lengths, distortions and chemical environments.

## Acknowledgments

This work was carried out for its experimental part at SSRL, which is a facility of Stanford University funded by the Department of Energy, USA, and for its theoretical part at INFN-LNF and BSRF-IHEP. Financial support was provided by MURST, Italy (project *Crystal-chemical, kinetic and thermodynamic aspects of minerals*), and by the *100-Talent Research Program* of the Chinese Academy of Sciences and the *Outstanding Youth Fund* (10125523) of the National Natural Science Foundation of China (ZYW). The Italian authors thank the entire SSRL staff for its experimental assistance, and J-L Robert for providing the synthetic micas.

## References

- [1] 2001 *Proc. XAFS XI Conf. (Ako, Japan, 2000)* *J. Synchrotron Radiat.* **8** and references therein  
Mottana A 2003 X-ray and inner-shell processes *19th Int. Conf. on X-ray and Inner-Shell Processes*  
ed A Bianconi, A Marcelli and N L Saini (New York: American Institute of Physics CP 652)
- [2] Mottana A, Robert J L, Marcelli A, Giuli G, Della Ventura G, Paris E and Wu Z Y 1997 *Am. Mineral.* **82** 497  
Mottana A, Marcelli A, Cibin G and Dyar M D 2002 *Rev. Mineral. Geochem.* **46** 371
- [3] Li D, Bancroft G M, Fleet M E, Feng X H and Pan Y 1995 *Am. Mineral.* **80** 432
- [4] Ildelfonse Ph, Cabaret D, Sainctavit Ph, Calas G, Flank A M and Lagarde P 1998 *Phys. Chem. Minerals* **25** 112
- [5] Poe B, Seifert F, Sharp T and Wu Z Y 1997 *Phys. Chem. Minerals* **24** 477
- [6] Wu Z Y, Romano C, Marcelli A, Mottana A, Cibin G, Della Ventura G, Giuli G, Courtial P and Dingwell D B 1999 *Phys. Rev. B* **60** 9216
- [7] Wu Z Y, Xian D C, Natoli C R, Marcelli A, Mottana A and Paris E 2001 *Appl. Phys. Lett.* **79** 1918
- [8] Rehr J J and Ankudinov A L 2003 *J. Synchrotron Radiat.* **10** 43
- [9] Natoli C R, Benfatto M, Della Longa S and Hatada K 2003 *J. Synchrotron Radiat.* **10** 26
- [10] Waychunas G A, Apter M J and Brown G E Jr 1983 *Phys. Chem. Minerals* **10** 1
- [11] Waychunas G A 1987 *Am. Mineral.* **72** 89
- [12] Bianconi A 1988 *X-ray Absorption: Principles, Applications, Techniques of EXAFS, SEXAFS, XANES*  
ed D C Konigsberger and R Prins (New York: Wiley)
- [13] Takeda H and Burnham C W 1969 *Mineral. J. Japan* **6** 102
- [14] Hazen R M and Burnham C W 1973 *Am. Mineral.* **58** 889
- [15] Cruciani G and Zanazzi P F 1994 *Am. Mineral.* **79** 289
- [16] Oberti R, Ungaretti L, Tlili A, Smith D C and Robert J L 1993 *Am. Mineral.* **78** 1290
- [17] Lee P A and Pendry J B 1975 *Phys. Rev. B* **11** 2795
- [18] Natoli C R, Benfatto M, Brouder C, Ruiz Lopez M Z and Foulis D L 1990 *Phys. Rev. B* **42** 1944  
Tyson T A, Hodgson K O, Natoli C R and Benfatto M 1992 *Phys. Rev. B* **46** 5997
- [19] Durham P J, Pendry J B and Hodges C H 1982 *Comput. Phys. Commun.* **25** 193
- [20] Durham P J 1988 *X-ray Absorption: Principles, Applications, Techniques of EXAFS, SEXAFS, XANES* ed  
D C Konigsberger and R Prins (New York: Wiley)
- [21] Lee P A and Beni G 1977 *Phys. Rev. B* **15** 2862
- [22] Mattheiss L 1964 *Phys. Rev. A* **134** 970
- [23] Clementi E and Roetti C 1974 *At. Data Nucl. Data Tables* **14** 177
- [24] Wille L T, Durham P J and Sterne P A 1986 *J. Physique Coll.* **47** C8 43
- [25] Natoli C R *et al* 1990 *Phys. Rev. B* **42** 1944
- [26] Fuggle J C and Inglesfield J E 1992 *Unoccupied Electronic States (Topics in Applied Physics)* (Berlin: Springer)  
p 347, appendix B
- [27] Norman J G 1974 *Mol. Phys.* **81** 1191
- [28] Wu Z Y, Marcelli A, Mottana A, Giuli G, Paris E and Seifert F 1996 *Phys. Rev. B* **54** 2976
- [29] Sharp T, Wu Z Y, Seifert F, Poe B, Doerr M and Paris E 1996 *Phys. Chem. Minerals* **23** 17–24
- [30] Benfatto M, Solera J A, Chaboy J, Proietti M G and Garcia J 1997 *Phys. Rev. B* **56** 2447
- [31] Ruckman M W, Reisfeld G, Jisrawi N M, Weinert M, Strongin M, Wiesmann H, Croft M, Sahiner A, Sills D and Ansari P 1998 *Phys. Rev. B* **57** 3881
- [32] van Aken P A, Wu Z Y, Langenhorst F and Seifert F 1999 *Phys. Rev. B* **60** 3815